Optimal Operation of Smart Houses by a Real-time Rolling Horizon Algorithm

Nikolaos G. Paterakis
Eindhoven University of Technology,
The Netherlands
n.paterakis@tue.nl

Iliana N. Pappi and João P. S. Catalão
FEUP, Porto, UBI, Covilha, and INESC-ID, IST, Univ. Lisbon, Lisbon, Portugal
iliananpappi@gmail.com; catalao@ubi.pt

Ozan Erdinc
Yildiz Technical University, Istanbul, Turkey, and INESC-ID, IST, Univ. Lisbon, Lisbon, Portugal
oerdinc@yildiz.edu.tr

***Abstract*—In this paper, a novel real-time rolling horizon optimization framework for the optimal operation of a smart household is presented. A home energy management system (HEMS) model based on mixed-integer linear programming (MILP) is developed in order to minimize the energy procurement cost considering that the household is enrolled in a dynamic pricing tariff scheme. Several assets such as a photovoltaic (PV) installation, an electric vehicle (EV) and controllable appliances are considered. Additionally, the energy from the PV and the EV can be used either to satisfy the household demand or can be sold back to the grid. The uncertainty of the PV production is estimated using time-series models and performing forecasts on a rolling basis. Also, appropriate distribution is used in order to model the uncertainty related to the EV. Besides, several parameters can be updated in real-time in order to reflect changes in demand and consider the end-user's preferences. The optimization algorithm is executed on a regular basis in order to improve the results against uncertainty.**

***Index Terms*—demand response; energy management systems; electric vehicle; photovoltaics; real-time pricing; real-time optimization; rolling optimization; uncertainty.**

I. Nomenclature

The main notation that is used throughout this study is concentrated in Tables I-III. Other symbols are defined where they appear.

TABLE I
Indices & Sets

$card()$	cardinality of a set.
h (H)	index (set) of optimization repetition interval.
m (M)	index (set) of controllable appliances.
p (P^m)	index (set) of operating phases of appliances.
t (T)	index (set) of time periods.
τ $([H^S, H^E] \cup \{T \mid t \leq h\})$	index (dynamic set) of time used in forecasting.
t' $((h, card(H)))$	index (dynamic set) of the time left to the end of the horizon.

TABLE II
Decision Variables

C_h	energy procurement cost in optimization repetition h (€).
$P^A_{m,t}$	power drawn from appliance m in period t (kW).
P^b_t	power drawn from the grid in period t (kW).
P^s_t	total power injected back to the grid in period t (kW).
$P^{EV,c}_t$	charging power of the EV in period t (kWh).
$P^{EV,d}_t$	discharging power of the EV in period t (kW).
$P^{x,s}_t$	power injected back to the grid from $x = \{EV, PV\}$ in period t (kW).
$P^{x,u}_t$	power used to cover house load from $x = \{EV, PV\}$ in period t (kW).
SOE^{EV}_t	state-of-energy of the EV in period t (kWh).
u^{EV}_t	binary variable – 1 if $x = \{EV, G\}$ is charging/power is drawn from the grid, else 0.
$u^{ph}_{m,p,t}$	binary variable – 1 if appliance m is in phase p in period t, else 0.
$y^{ph}_{m,p,t}$	binary variable – 1 if appliance m is entering phase p in period t, else 0.
$z^{ph}_{m,p,t}$	binary variable – 1 if appliance m is finishing phase p in period t, else 0.

II. Introduction

The residential sector is responsible for approximately 40% of the total energy consumption worldwide. As a result, the residential end-user premises have been in the center of attention for designing suitable incentive and price based demand response (DR) programs recently. In order to effectively exploit the flexibility that several appliances located at the end-user premises present and to facilitate the automated response to the DR signals, the penetration of home energy management systems (HEMS) is showing an increasing tendency. Several industrial applications have already been developed, while a number of academic studies are devoted to designing effective HEMS structures taking into account several parameters such as the compromise between the end-user comfort and the response to the DR signals, as well as the exploitation of the price based DR in order to minimize the energy procurement cost of the household.

In the recent technical literature, two main categories of studies related to the HEMS may be distinguished. The first category evaluates the day-ahead operation of the HEMS structure such as in [1], [2]. The second category of technical studies focuses on the actual operation of the HEMS. In this second group of HEMS applications, the intermittent behavior of renewable DG units was considered together with other uncertainties in [3] by adapting the offline scheduling to runtime dynamic scheduling. De Angelis et al. [9] proposed a Mixed-Integer Linear Programming (MILP) model of a HEMS aiming to minimize the operational cost, taking user-comfort oriented electrical and thermal constraints into account. The study in [4] considered the impact of several possible system interruptions, such as adding a new task, adding a critical load and EV connection or disconnection by adjusting its future time dynamically. However, [4] neglects bi-directional power flows. A rolling optimization based on mixed-integer nonlinear programming (MINLP) focusing particularly on load modeling was also presented in [5]. Nevertheless, the scalability of nonlinear models is debatable.

TABLE III
PARAMETERS

CR^{EV}	maximum charging rate of the EV (kW).
DR^{EV}	maximum discharging rate of the EV (kW).
E_1^r	minimum readily available state-of-energy the r-th time the EV is plugged in (kWh).
E_2^r	state-of-energy that is ideally required by the driver upon departure the r-th time the EV is plugged in (kWh).
$EV_{h,t}^{status}$	binary parameter – 1 if EV is plugged in period t in optimization round h.
$L_{h,t}$	consumption of uncontrollable loads in period t in optimization round h (kW).
M_m	number of times appliance m operates during the day.
N	limit of power drawn/injected to the grid (kW).
$P_{m,p}^{ph}$	power of appliance m in phase p (kW).
$P_{h,t}^{PV,a}$	available PV production in period t in optimization round h (kW).
$SOE_{h,t}^{EV,max}$	maximum state-of-energy of the EV (kWh).
$SOE_{h,t}^{EV,min}$	minimum state-of-energy of the EV (kWh).
$T_{m,p}^{dur}$	duration of phase p of appliance m (number of periods).
$T_{h,m}^{E}$	earliest period appliance m can start operating (known in optimization round h).
$T_{h,m}^{L}$	latest period appliance m must have operated (known in optimization round h).
ΔT	duration of optimization interval (h).
$\eta^{EV,c}$	charging efficiency of the EV (%).
$\eta^{EV,d}$	discharging efficiency of the EV(%).
λ_t	energy price at period t (€/kWh).
μ^r	mean of normal distribution the r-th time (period).
ξ_1^r	minimum limit of truncated (period).
ξ_2^r	maximum limit of truncated (period).
σ^r	standard deviation of normal distribution the r-th time (period).

Finally, the stochastic nature of household energy management was considered through a three-step HEMS structure, firstly analyzing the status of appliances, then providing stochastic scheduling and lastly initiating the control actions in real-time in [6]. However, rolling adaptation of HEMS through new values of uncertain parameters was not considered in [6].

The main contribution of this study is twofold:

1. A novel real-time rolling horizon optimization framework is presented. The optimization problem of the HEMS is formulated as a MILP model aiming to minimize the energy procurement cost on a daily basis. A fully-fledged smart household is considered, incorporating a PV installation, an EV and controllable appliances. Additionally, bi-directional power flow is considered by means of taking into account the Distributed Generation (DG)-to-home (DG2H), DG-to-grid (DG2G) and EV-to-home (EV2H), EV-to-grid (EV2G) capabilities.
2. The inherent uncertainty in the PV production is captured by performing forecasts based on time series models also on a rolling basis. Moreover, the uncertainty related to the EV departure time is tackled by means of probability distribution functions. Furthermore, the end-user can alter in real-time the preferences over the operation of controllable appliances, while the estimation of the uncontrollable load consumption can be updated in order to provide a better estimation of the end-user's load.

The remainder of the paper is organized as follows: Section III describes the methodology. Afterwards, in order to test the proposed approach a case study is studied in Section IV. Finally, conclusions are drawn in Section V.

III. METHODOLOGY

A. Real-time optimization algorithm

The forecasting of the PV production is based on time series models [7]. Firstly, historical data of appropriate time granularity are collected for the variable that needs to be forecasted. Then, in order to stabilize the variance of the time series, the logarithmic transformation is applied to the original data. Subsequently, an ARIMA model is fitted to the logarithmically transformed time series.

In order to perform forecasts on a rolling basis, each time new data are available the initially fitted ARIMA model is tested as regards its capability to be accurately used to forecast the future values of the random variable utilizing the emerging time series. The proposed approach is described by Algorithm 1. First, it is essential to elaborate the different time indices that are utilized. There are two main indices $t \in T$ and $h \in H$ which stand for the time intervals of the optimization horizon and the time interval in which optimization is performed, respectively. Furthermore, the time index $\tau \in [H^S, H^E] \cup T$ is used in order to perform forecasts for the PV power production. Finally, time index t' refers to the future values of t with respect to h. It should be noted that although at each iteration h a looking-forward multi-period optimization is performed, the decision that is implemented refers to period t which coincides with h. On the same line, the decision variables are fixed to their optimal values for the periods that belong to the past with respect to the current optimization iteration.

B. Formulation of the optimization problem

In their previous studies [1], [2], the Authors have presented the deterministic optimization problem of a HEMS under hourly-varying pricing. However, the constraints of the problem must be modified in order to be used in a real-time rolling horizon optimization framework. Detailed explanations for the equations can be found in [1], [2].

Algorithm 1: Real-time optimization algorithm

1: set the parameters of the HEMS, obtain historical PV production data and the retailer 24-h price signal
2: **if** $EV_{1,1}^{status} = 1$ **do**
3: $SOE_1^{ESS} \leftarrow SOE^{ESS,ini}$
4: **end if**
5: **for** $h = 1 \rightarrow card(H)$ **do**
6: **if** new available PV production data is available **do**
7: fit ARIMA model (1) to $\psi'_\tau, \tau \in [H^S, H^E] \cup \{T | t \leq h\}$
8: perform forecast $f_{t'}, t' \in (h, card(H))$ for available PV power production
9: **for** $t = 1 \rightarrow card(T)$ **do**
10: **if** $t > h$ **do**
11: $P_{h,t}^{PV,a} \leftarrow f_{t'}, t \equiv t'$
12: **else**
13: $P_{h,t}^{PV,a} \leftarrow \psi'_\tau, t \equiv \tau$
14: **end if**
15: **end for**
16: **else**
17: $P_{h,t}^{PV,a} \leftarrow P_{h-1,t}^{PV,a}$
18: **end if**
19: update parameters: $EV_{h,t}^{status}, L_{h,t}, SOE_{h,t}^{EV,min}$
20: **SOLVE** optimization problem minimize (1), s.t. (2)-(27).
21: **for** $t = 1 \rightarrow card(T)$ **do**
22: **if** $t \leq h$ **do**
23: fix the values of the decision variables to their optimal value
24: **end if**
25: **end for**
26: **end for**

Although the time span of the objective function is the whole set of periods of the optimization horizon, the decision variables are optimized for the upcoming periods with respect to the current optimization repetition h since the values of the variables before that interval are fixed to their optimal values by Algorithm 1.

B.1. Objective function

The objective function of the optimization problem (1) is to minimize the energy procurement cost of the smart household at each optimization repetition.

$$C_h = \sum_t [(P_t^b - P_t^s) \cdot \lambda_t \cdot \Delta T] \quad (1)$$

B.2. Grid power transactions and power balance

Constraints (2) and (3) enforce the fact that at each time interval energy is either drawn by the household or is injected back to the grid.

$$P_t^b \leq N \cdot u_t^G, \forall t \geq h \quad (2)$$

$$P_t^s \leq N \cdot (1 - u_t^G), \forall t \geq h \quad (3)$$

The energy that is sold back to the grid may come from the PV or the EV battery when the EV is plugged-in.

$$P_t^s = P_t^{PV,s} + P_t^{EV,s}, \forall t \geq h \quad (4)$$

The power balance at each time interval is represented by equation (5).

$$P_t^b + P_t^{PV,u} + P_t^{EV,u} = L_{h,t} + P_t^{EV,c}, \forall t \geq h \quad (5)$$

B.3. Photovoltaic constraints

The allocation of the total available power that comes from the PV installation is defined by equation (6).

$$P_{h,t}^{PV,a} = P_t^{PV,s} + P_t^{PV,u}, \forall t \geq h \quad (6)$$

B.4. Electric vehicle

The EV is modeled using constraints (7)-(13). The EV arrival and departure time are two important parameters for the HEMS since they affect the optimal V2H, V2G and charging decisions. It should be noted that since the optimization is realized in discrete intervals, if the EV arrives between two optimization repetitions, then the parameter is updated in the next optimization round.

$$P_t^{EV,c} \leq CR^{EV} \cdot u_t^{EV}, \forall t \geq h, \text{ if } EV_{h,t}^{status} = 1 \quad (7)$$

$$P_t^{EV,d} \leq DR^{EV} \cdot (1 - u_t^{EV}), \forall t \geq h, \text{ if } EV_{h,t}^{status} = 1 \quad (8)$$

$$P_t^{EV,u} + P_t^{EV,s} = P_t^{EV,d} \cdot \eta^{EV,d}, \forall t \geq h, \text{ if } EV_{h,t}^{status} = 1 \quad (9)$$

$$SOE_{h,t}^{EV,min} \leq SOE_t^{EV} \leq SOE^{EV,max}, \forall t \geq h, \text{ if } EV_{h,t}^{status} = 1 \quad (10)$$

$$SOE_t^{EV} = SOE_{t-1}^{EV} + \left(P_t^{EV,c} \cdot \eta^{EV,c} - P_t^{EV,d}\right) \cdot \Delta T, \forall t > 1, t \geq h, \text{ if } EV_{h,t}^{status} = EV_{h,t-1}^{status} = 1 \quad (11)$$

$$SOE_t^{EV} = SOE^{EV,ini} + \left(P_t^{EV,c} \cdot \eta^{EV,c} - P_t^{EV,d}\right) \cdot \Delta T, \text{ if } t = h \text{ and } EV_{h,t}^{status} - EV_{h,t-1}^{status} = 1 \quad (12)$$

$$P_t^{EV,c}, P_t^{EV,d}, P_t^{EV,u}, P_t^{EV,s}, SOE_t^{EV}, u_t^{EV} = 0, \text{ if } EV_{h,t}^{status} = 0 \quad (13)$$

Although by updating the $EV_{h,t}^{status}$ in real-time the plug in time can be immediately known, there is still uncertainty as regards the time at which the driver departs. It is important to accurately estimate the EV departure time since a certain SOE level may be required in order to satisfy the commuting needs of the end-user. To confront this issue, in this paper it was considered that the departure of the EV follows a truncated normal distribution [8] with a standard deviation σ and a mean μ derived from historical car usage data and depends on the time that the EV is plugged in.

Based on the cumulative distribution function appropriate values for the $SOE_{h,t}^{EV,min}$ are calculated using (14).

$$SOE_{h,t}^{EV,min} = E_1^r + (E_2^r - E_1^r) \cdot \frac{1}{\sigma^r \sqrt{2\pi}} \sum_{v=\xi_1^r}^{t} \left(e^{\frac{-(v-\mu^r)^2}{2(\sigma^r)^2}} \right), \quad \forall h \leq t \leq \xi_2^r \quad (14)$$

B.5. Controllable appliances

The controllable appliances (e.g. washing-machine and dishwasher) are modeled using constraints (15)-(21).

$$P_{m,t}^A = P_{m,p}^{ph} \cdot u_{m,p,t}^{ph}, \forall m, t \in [T_{h,m}^E, T_{h,m}^L] \quad (15)$$

$$\sum_p u_{m,p,t}^{ph} \leq 1, \forall m, t \in [T_{h,m}^E, T_{h,m}^L] \quad (16)$$

$$y_{m,p,t}^{ph} = z_{m,p,(t+T_{m,p}^{dur})}^{ph}, \forall m, p, t \in [T_{h,m}^E, T_{h,m}^L] \quad (17)$$

$$y_{m,p,t}^{ph} - z_{m,p,t}^{ph} = u_{m,p,t}^{ph} - u_{m,p,(t-1)}^{ph}, \forall m, p, t \in [T_{h,m}^E, T_{h,m}^L], \text{ if } t > 1 \quad (18)$$

$$z_{m,p,t}^{ph} = y_{m,(p+1),t}^{ph}, \forall m, p, t \in [T_{h,m}^E, T_{h,m}^L] \quad (19)$$

$$\sum_{t \in [T_{h,m}^E, T_{h,m}^L]} y_{m,p,t}^{ph} = M_m, \forall m, p \quad (20)$$

$$P_{m,t}^A, y_{m,p,t}^{ph}, z_{m,p,t}^{ph}, u_{m,p,t}^{ph} = 0, \forall t \notin [T_{h,m}^E, T_{h,m}^L] \quad (21)$$

The reason why these equations are not defined for $t \geq h$ similar to the rest of the constraints is that the intertemporal characteristics which describe these equations span several periods in the past. On the contrary, in the previous constraints, either no intertemporal relations exist (e.g. power balance constraint) or the intertemporal characteristics are limited to the immediately previous period of the one the optimization occurs in (e.g. SOE of EV).

IV. Numerical Application

A. Description of the case study

In order to demonstrate the proposed algorithm, a numerical test case is studied in this section. The optimization horizon is 96 15-minute intervals and the real-time optimization is performed in each period for the remaining periods. A 4-member household located in Belgium is considered, comprising typical uncontrollable appliances, a dishwasher and a washing machine which can be optimally scheduled considering the preferences of the end-users. The inflexible load of the household is given in Fig. 1 and is generated based on a modified version of the model presented in [9]. The cycle profiles of the controllable appliances are presented in [2], while their operation must be completed between 12pm and 9pm. Additionally, a PV installation with a rated capacity of 3 kW is considered. In order to forecast the PV production on 16/6/2015, historical data with 15-minute granularity spanning from 9/6/2015 to 15/6/2015 are first obtained by the Belgian Transmission System Operator ELIA [10]. The historical time series is depicted in Fig. 2. In practice, in order to improve the accuracy of the forecasting, the PV power production time series is processed in order to exclude the periods in which PV power is zero (night time), i.e. the time intervals from 8:45pm to 6:15am. Subsequently, the ARIMA model (22) is estimated for the modified time series. Due to the fact that in the modified time series each day comprises 57 time intervals, the backshift operator B^{57} considers the daily periodicity of the PV production.

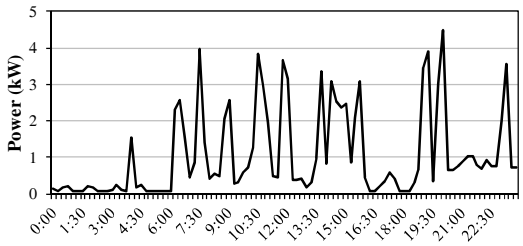

Fig. 1. Inflexible load profile.

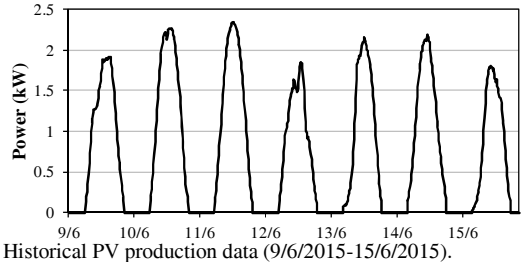

Fig. 2. Historical PV production data (9/6/2015-15/6/2015).

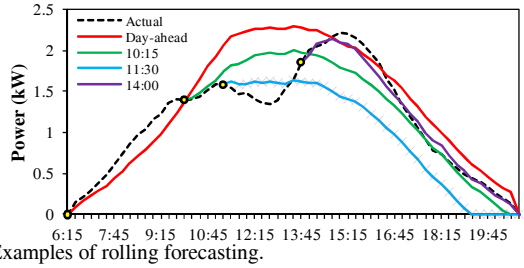

Fig 3. Examples of rolling forecasting.

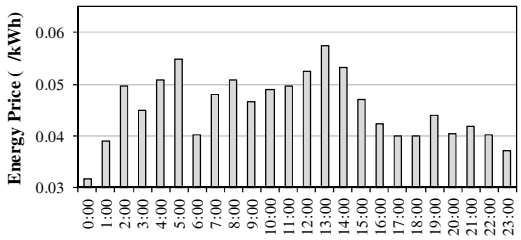

Fig. 4. Energy price signal.

$$\psi_\tau = \frac{1}{(1-B^1)(1-B^{57})} \cdot \frac{(1-\theta_1 B^1+\theta_2 B^2-\theta_3 B^3-\theta_4 B^4-\theta_9 B^9-\theta_{64} B^{64})}{(1-\varphi_1 B^1+\varphi_2 B^2-\varphi_3 B^3-\varphi_4 B^4-\varphi_5 B^5-\varphi_{57} B^{57})} \cdot \frac{(1-\theta_{57} B^{57})}{(1-\varphi_{12} B^{12}-\varphi_{57} B^{57})} \cdot \varepsilon_\tau + c \quad (22)$$

For each repetition of the forecasting, i.e. every 15 minutes, the same ARIMA model has been found to lead to uncorrelated residuals. However, the parameters of the model need to be adjusted. In Fig. 3 the actual PV production, the day-ahead and the results of some rolling intra-day forecasts are demonstrated. By observing the historical data and the day under investigation, it may be concluded that it presents an irregularity in comparison with the typical bell shape of the PV production. As a result, the day-ahead forecast presents a mean absolute percentage error (MAPE) of 28%. On the other hand, as the intra-day forecasts are updated every 15 minutes and the optimal decisions at each step refer to the next 15-minutes, the MAPE falls to 4%.

The EV considered in this case study is a Nissan LEAF which is equipped with a 24 kWh battery and a range of 84 miles, while the charger maximum power is 6.6 kW [11]. At the beginning of the optimization horizon the EV is connected at the charging point with an initial SOE of 8 kWh. It is assumed that according to available data related to the driving behavior of the user, the EV departure time in the morning follows a normal distribution with a mean at 7am and a standard deviation of 15 min, truncated between 6:30am and 9am. Given that 66% of the commuting trips in Belgium are shorter than 11.78 miles [12] which corresponds to 3.36 kWh, the minimum level of SOE is set to 4 kWh. It is typical to assume that ideally the driver desires to have the EV fully charged at the time he/she decides to depart. Even though it is possible to estimate when the EV will depart using a probability distribution based on the end-user's habits, the exact departure time cannot be known. As a result, it is probable that the HEMS optimization will not sufficiently charge the battery of the EV unless a constraint is enforced. To perform so, a minimum SOE is calculated by multiplying the cumulative distribution function of the departure time with the effective capacity of the battery (rated capacity minus the minimum imposed SOE). Also, for the purposes of the real-time simulation the EV returns at a random time period (a period between 6pm to 6:15pm and a SOE of 12 kWh were randomly selected) and a new estimation regarding the next departure time is made. In this case, a truncated normal distribution (7:30pm- 9:15pm) with a mean at 8:30 pm and a standard deviation of 30 minutes was used. Regarding the pricing of the energy, a net metering approach is adopted and therefore, the prices of buying and selling energy are identical. The household is enrolled to a time-varying pricing program that prices the end-users according to the day-ahead market prices similar to [13], therefore there is no uncertainty associated with the electricity prices. The day-ahead price signal in the Belgian market on 16/6/2015 is displayed in Fig. 4 [14].

B. Simulation results

The proposed optimization algorithm was implemented in GAMS and the optimization problems were solved using the commercial solver CPLEX. The solution time on a modern laptop computer employing an i7 processor clocking at 2.4 GHz and 4GB of RAM is 0.20 sec per optimization execution, while the time required in order in order to estimate the ARIMA parameters utilizing the ECOTOOL MATLAB toolbox [15] is approximately 0.59 sec.

First of all, the relevant results regarding the scheduling of EV charging and discharging by the real-time algorithm are illustrated in Fig. 5. Initially, the EV is at home and plugged-in, while it is estimated to leave between 6:30am and 9am. According to the relevant cumulative distribution function the minimum SOE should be kept above a monotonically increasing value between 6:30am and 8am. The car departs at 7:15am. In that period its SOE should be at least 22.54 kWh, yet, it is fully charged. The optimization performed at 0:00am (and all the optimization rounds that are executed up to 7:15 am) consider that the car is available until 9am. Subsequently, for the optimization rounds that take place between 7:15am and 6:00pm, the period at which the car is plugged in for the second time, the EV constraints are relaxed. As soon as the car is plugged in, another estimation regarding the next departure time is performed. As a result, for the optimization rounds until 9:15pm, the car would not be available after 9:15pm and a minimum SOE limit is imposed. However, in real-time, the driver does not depart and as a result the EV battery is fully charged at 9:15pm and since the next departure time is outside the scope of the optimization horizon, the EV is discharged from 9:15pm to 11:45pm.

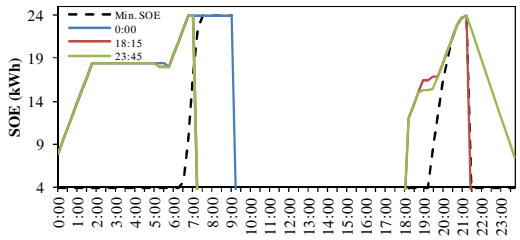

Fig. 5. EV SOE in different optimization executions.

In Fig. 6, the real-time scheduling of the washing machine and the dishwasher that are considered flexible appliances is demonstrated. Given the PV power production forecast that is performed at 6:30am, the algorithm decides to allocate the washing machine between 12pm and 1:15pm, while the dishwasher is scheduled to operate between 5pm and 6:30pm. This decision is related to two facts: first, the loads are assigned to periods in which the uncontrollable load of the household presents relatively low consumption levels, and second, the predicted power that is available from the PV in these periods, leads to a smaller net load. At the optimization execution that takes place at 12:15pm, the washing machine has already operated for 15 minutes. Additionally, since the updated PV production forecast predicts lower PV generation available between 5pm and 6:30pm, the operation of the dishwasher is shifted earlier, starting at 12:15pm in order to exploit both the relatively higher PV production and the lower uncontrollable load consumption.

The net power exchange between the household and the grid are illustrated in Fig 7. for the day-ahead scheduling (optimization execution at 12am) and for the last execution of the algorithm (11:45pm). It can be noticed that there are mismatches during the noon time between the power that is injected from the grid to the household and vice versa, due to the fact that the day-ahead PV production forecast has been rather optimistic in comparison with the actual PV production. As a result, more energy needs to be bought in real-time in order to satisfy the household load and less excessive energy is available to be sold by the household.

V. Conclusions

In this paper, a novel real-time rolling horizon optimization framework for the optimal operation of a HEMS aiming to minimize its energy procurement cost was developed.

The analysis of the case study demonstrated the following:

1. The fact that incorporating new information regarding the actual production of PV and performing forecast on a rolling basis reduces average error, allowing the proposed algorithm to converge to a daily operational cost that is practically equal to the one obtained for perfect knowledge of PV production.
2. The uncertainty related to the EV is revealed to be the key factor that affects daily energy procurement cost of the household.

The proposed approach can be further expanded by considering other models in order to capture the uncertainty of the EV, which will be the subject of future research.

VI. Acknowledgement

This work was supported by FEDER funds through COMPETE and by Portuguese funds through FCT, under FCOMP-01-0124-FEDER-020282 (Ref. PTDC/EEA-EEL/118519/2010), UID/CEC/50021/2013 and SFRH/BPD/103744/2014. Also, the research leading to these results has received funding from the EU Seventh Framework Programme FP7/2007-2013 under grant agreement no. 309048 (project SiNGULAR).

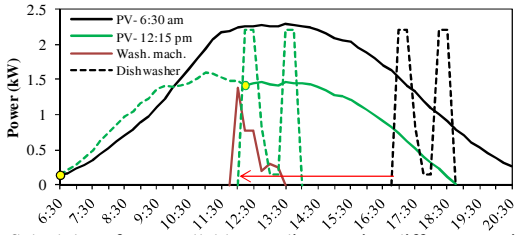

Fig. 6. Schedule of controllable appliances in different optimization executions.

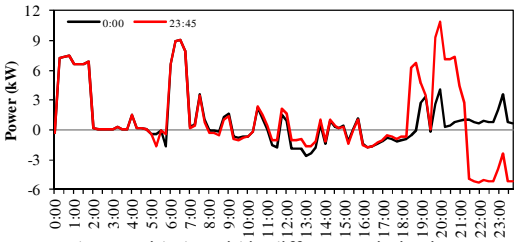

Fig. 7. Power exchange with the grid in different optimization executions.

VII. References

[1] O. Erdinc, N. G. Paterakis, T. D. P. Mendes, A. G. Bakirtzis, and J. P. S. Catalão, "Smart household operation considering bi-directional EV and ESS utilization by real-time pricing-based DR," *IEEE Trans. Smart Grid*, vol. 6, pp. 1281-1291, May 2015.

[2] N. G. Paterakis, O. Erdinc, A. G. Bakirtzis, J. P. S. Catalão, "Optimal household appliances scheduling under day-ahead pricing and load-shaping demand response strategies," IEEE Trans. Industrial Informatics, *in press*.

[3] X. Chen, T. Wei, and S. Hu, "Uncertainty aware household appliance scheduling considering dynamic electricity pricing in smart home," *IEEE Trans. Smart Grid*, vol. 4, pp. 932-941, June 2013.

[4] F. de Angelis, M. Boaro, D. Fuselli, S. Squartini, F. Piazza, and Q. Wei, "Optimal home energy management under dynamic electrical and thermal constraints," *IEEE Trans. Industrial Informatics*, vol. 9, pp. 1518-1527, Aug. 2013.

[5] S. Althaher, P. Mancarella, and J. Mutale, "Automated demand response from home energy management system under dynamic pricing and power and comfort constraints," *IEEE Trans. Smart Grid*, vol. 6, pp. 1874-1884, July 2015.

[6] C. Vivekananthan, Y. Mishra, and F. Li, "Real-time price based home energy management scheduler," *IEEE Trans. Power Systems*, vol. 30, pp. 2149-2159, July 2015.

[7] G. E. Box, G. M. Jenkins, and G. C. Reinsel, *Time Series Analysis: forecasting and control*. John Wiley & Sons, 2013.

[8] S.I. Vagropoulos, A.G. Bakirtzis, "Optimal bidding strategy for electric vehicle aggregators in electricity markets," *IEEE Trans. Power Systs*., vol. 28, pp. 4031-4041, Nov. 2013.

[9] Loughborough University Institutional Domestic Electricity Demand Model. [Online]. Available: http://hdl.handle.net/2134/5786

[10] Belgian Transmission System Operator ELIA. [Online]. Available: http://www.elia.be

[11] Plug-in electric vehicles. [Online]. Available: http://www.plugincars.com

[12] Karen Geruts (2014). *Modal choice for travel to work and school-Recent trends and regional differences in Belgium*. [Online]. Available: http://www.plan.be

[13] Ameren Illinois power smart pricing. [Online]. Available: http://www.powersmartpricing.org

[14] ENTSO-e transparency platform. [Online]. Available: http://transparency.entsoe.eu

[15] D. J. Pedregal, J. Contreras, and A. A. Sanchez de la Nieta, "ECOTOOL: a general MATLAB forecasting toolbox with applications to electricity markets," in *Handbook of Networks in Power Systems I*. Springer, 2012.